Excited-State Dynamics of Water-Soluble Polythiophene Derivatives: Temperature and Side-Chain Length Effects

ARTICLE *in* THE JOURNAL OF PHYSICAL CHEMISTRY B · NOVEMBER 2012

Impact Factor: 3.3 · DOI: 10.1021/jp304526h · Source: PubMed

THE JOURNAL OF PHYSICAL CHEMISTRY B

Article

pubs.acs.org/JPCB

Excited-State Dynamics of Water-Soluble Polythiophene Derivatives: Temperature and Side-Chain Length Effects

Ying-Zhong Ma,*[,†] Robert W. Shaw,[†] Xiang Yu,[†] Hugh M. O'Neill,[§] and Kunlun Hong*[,‡]

[†]Chemical Sciences Division, Oak Ridge National Laboratory, P.O. Box 2008, Oak Ridge, Tennessee 37831, United States

[‡]Center for Nanophase Materials Sciences, Oak Ridge National Laboratory, P.O. Box 2008, Oak Ridge, Tennessee 37831, United States

[§]Center for Structural Molecular Biology, Biology & Soft Matter Division, Oak Ridge National Laboratory, P.O. Box 2008, Oak Ridge, Tennessee 37831, United States

ABSTRACT: We report synthesis and detailed spectroscopic study of three water-soluble polythiophene derivatives with distinct homologous oligo(ethylene oxide) side-chain lengths and lower critical solution temperatures (LCSTs). The linear absorption spectra exhibit reversible shifts and broadening with the variation of their aqueous solution temperature, whereas the corresponding steady-state fluorescence emission spectra were found to show negligible shifts and only minor changes in their line shape. Measurements of picosecond time-resolved fluorescence at chosen emission wavelengths reveal a strong dependence of the isotropic decays on both side-chain length and aqueous solution temperature. With lengthening of the side chain, the isotropic decays become not only remarkably slow but also increasingly complex. Except for the polymer with the shortest side chain, significant acceleration of the isotropic decays was found when the solution temperature was raised to the corresponding LCSTs and beyond, which further causes formation of large aggregates as evident by the physical appearance change from clear solutions to turbid suspensions. Direct evidence for a temperature-induced change of polymer chain conformation was obtained through measurements of time-resolved fluorescence anisotropies, which are characterized by a substantial increase of the initial values from ~0.2 to 0.4 and the appearance of a pronounced fast decay component with an estimated lifetime of 36 ps. The high initial anisotropy of ~0.4 observed for the two polymers with longer side-chains above their LCSTs suggests that the polymer chains are highly ordered in the aggregates. The observed effects of side-chain length and solution temperature are discussed by considering the conformational relaxation of the polymer backbones and occurrence of interchain energy transfer.

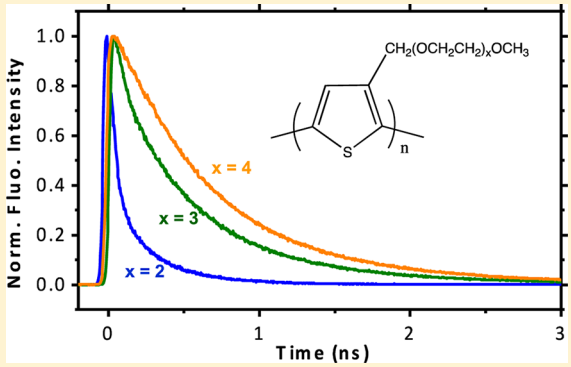

INTRODUCTION

Polythiophenes have emerged as one of the most versatile families of conjugated polymers because of their excellent optoelectronic properties, high charge carrier mobility, good chemical/thermal stability, and tunable solubility in organic solvents.[1−3] These unique properties have enabled a wide range of applications such as organic field-effect transistors,[4−6] organic solar cells,[7] chemical and optical sensors,[8] and electrochromic devices.[9] A particularly exciting advance involves use of a poly(3-hexylthiophene) (P3HT) polymer as both light absorber and electron-donating molecule in bulk heterojunction solar cells, which has enabled a high power conversion efficiency of ~5%.[10] These novel properties and exciting applications have stimulated extensive efforts in recent years to understand their optical properties,[11−13] as well as the nature of their elementary photoexcitations,[14] electronic excited-state dynamics,[15−18] and exciton migration and photoinduced charge separation in the presence of a fullerene electron acceptor such as [6,6]-phenyl C_{60} butyric acid methyl ester (PCBM).[19−23]

The insolubility of polythiophene polymers in water and aqueous media hinders their applications in biological environments[24] and prevents environmentally friendly processing.[25] A general strategy to enable their water solubility is to attach hydrophilic side chains with either charged or neutral groups to the hydrophobic backbones of polythiophenes.[26] The hydrogen-bonding interactions between these side chains and surrounding water molecules serve as the driving force for aqueous solubilization of these synthetic polythiophene derivatives.[27−29] An even more remarkable thermoresponsive property with a material-specific lower critical solution temperature (LCST) can further arise from the amphiphilic character of these synthetic polymers, i.e., coexistence of hydrophobic backbones and hydrophilic side chains. Owing to a rapid conformational change with increasing temperature,[28] these polymers are soluble in water below their characteristic LCSTs but aggregate and/or precipitate above the LCSTs. The

Received: May 9, 2012
Revised: November 9, 2012
Published: November 9, 2012

Scheme 1

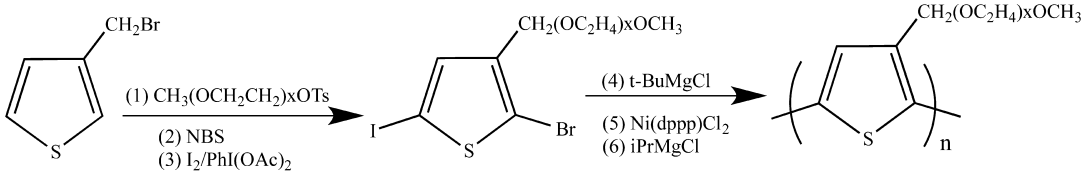

corresponding conformational changes have been studied extensively for various thermoresponsive polymers (see refs 29 and 30, and relevant references cited therein). For instance, through application of a dynamic light scattering technique, Lutz and co-workers found that the thermoresponsive copolymers of 2-(2-methoxyethoxy)ethyl methacrylate and oligo(ethylene glycol) methacrylate adopt mostly a coiled conformation in water with a hydrodynamic radius of ∼3.7 nm below the LCST but form large aggregates with a hydrodynamic radius of ∼300 nm above the LCST. These large aggregates are further assumed to form stable mesoglobules that result from aggregation of collapsed dehydrated chains.[28,29] Similar sizes of aggregates have also been observed above the LCST for poly(*N*-isopropylacrylamide), poly(*N*,*N*-diethylacrylamide), and poly(vinylmethyl ether).[31−33] In contrast, little is known about the molecular organization in aggregates, specifically, whether the polymer molecules adopt backbone conformations that are significantly different from their solubilized forms. Our understanding about the spectral characteristics and electronic excited-state dynamics of the aggregates and how they are distinct from the solubilized polymers below the LCST is also limited. Picosecond time-resolved fluorescence and polarization measurements can provide useful insight into these poorly understood questions; the knowledge so gained will likely not only further our fundamental understanding about water-soluble polythiophene polymers in both solubilized and aggregated forms but also benefit the potential applications based on either their thermoresponsive properties or/and water solubility.

In this paper, we report synthesis of three poly(3-oligo(ethylene oxide)) thiophenes with distinct side-chain lengths, denoted hereafter as EO_x with x = 2, 3, and 4, which represents the number of repeating EO (ethylene oxide) groups. The different side-chain lengths provide control of both the water solubility and LCSTs. We found that the linear absorption spectra undergo fully reversible changes (spectral shift and broadening) with the variations of the aqueous solution temperature. The most drastic spectral changes were observed at the corresponding LCSTs with a concomitant appearance of solution turbidity. Picosecond time-resolved fluorescence anisotropy measurements at temperatures above LCSTs provide direct evidence for polymer backbone ordering in the aggregates and occurrence of interchain energy transfer. Significant effects of the side-chain length and solution temperature on the isotropic fluorescence decays were also identified.

MATERIALS AND METHODS

Polymer Synthesis and Sample Preparation for Spectroscopic Experiments. The polythiophene derivatives were synthesized based on the Kumada catalyst transfer polymerization, and the whole reaction is outlined in Scheme 1.[34] The polymers obtained were characterized using ^{1}H NMR and gel permeation chromatography (GPC), and the results are summarized in Table 1. For all spectroscopic measurements, the polymers were dissolved in deionized water, and fluorescence cuvettes with a 1-cm path length were used. Control of the sample temperature was realized using a thermostatted cuvette holder connected to either a thermoelectric heater/cooler or a water-circulating chiller. In either case, the sample temperature was monitored directly inside the cuvette holder using a thermocouple thermometer.

Table 1. Characteristics of the Water-Soluble Thiophene Polymers

polymer	molecular weight[a] (kg/mol)	repeat unit (n)	polydispersity[a]	regioregularity,[b] %
EO_2	6.5	30.0	1.21	96
EO_3	7.3	28.1	1.25	97
EO_4	7.8	25.7	1.19	97

[a]From GPC (obtained using a Waters 2690 system equipped with a 410 RI detector and two polystyrene gel columns (PLgel 5 μm MIXED-C) using THF as the eluent at a flow rate of 1.0 mL per min. The relative molecular weight was calibrated using standard polystyrene samples. [b]From ^{1}H NMR in $CDCl_3$ obtained using a Varian 500 MHz NMR at room temperature.

Measurements of Linear Absorption and Steady-State Fluorescence Emission Spectra. A Varian 5000 UV−vis−NIR absorption spectrometer was used to record the linear absorption spectra at different temperatures. The corrected fluorescence emission spectra were measured using a Fluorolog-3 spectrofluorometer upon excitation at 445, 427, and 410 nm for EO_2, EO_3, and EO_4, respectively. Typical bandwidths for the excitation and emission monochromators were 5 and 2 nm, respectively.

Measurements of Picosecond Time-Resolved Fluorescence and Anisotropy. A time-correlated single-photon-counting (TCSPC) apparatus based on an actively quenched single-photon avalanche photodiode (PDM 50CT module, Micro Photon Devices) connected to a PicoQuant TCSPC system (PicoHarp 300, Picoquant) was employed. An optical parametric amplifier pumped by a 250 kHz Ti:Sapphire regenerative amplifier was used as the excitation source. Excitation was at 490 nm with typically 150 fs (full width at half maximum, fwhm) pulse duration and <8 nJ pulse energy. Fluorescence emission was selected by using a 10 nm (fwhm) bandpass filter centered at 620 nm for EO_2 and EO_3 and at 589 nm for EO_4, which were chosen as close to the peak wavelengths of the fluorescence emission spectra as possible. The instrument response function (IRF) showed a fwhm of ∼40 ps as recorded at the excitation wavelength using a dilute water suspension of coffee creamer. A 4.0-ps channel time was

dx.doi.org/10.1021/jp304526h | J. Phys. Chem. B 2012, 116, 14451−14460

chosen, and typically more than 10 000 counts were collected in the peak channel to obtain an acceptable signal-to-noise ratio. Isotropic fluorescence data were collected by setting the polarization of the laser excitation at the magic angle (54.7°) with respect to an emission linear polarizer. Measurements of time-resolved fluorescence anisotropy involve collecting data for four polarization combinations of an excitation half-wave plate and an emission linear polarizer and calculating according to the following relationship:

$$r(t) = \frac{I_{VV}(t) - GI_{VH}(t)}{I_{VV}(t) + 2GI_{VH}(t)}$$

where $I_{VV}(t)$ and $I_{VH}(t)$ are the fluorescence decays measured with parallel and perpendicular polarizations, respectively. The G-factor was obtained by measuring two additional decays, $I_{HV}(t)$ and $I_{HH}(t)$, and calculating according to the relationship $G = \int I_{HV}(t)dt / \int I_{HH}(t)dt$.

RESULTS

Linear Absorption and Steady-State Fluorescence Emission Spectra. Figure 1a shows the linear absorption spectra recorded for EO_4 at multiple aqueous solution temperatures ranging from 32 °C to 80 °C. It is clearly evident that the linear absorption spectra are very sensitive to temperature. Even for this moderate temperature change, a red-shift as large as 35 nm and a clear spectral broadening occurred. We further noticed that both the spectral shift and broadening could be fully reversed by simply lowering the temperature to the initial value (Figure 1b). This reversible spectral change can be better seen through plotting the peak wavelengths of the absorption spectra as a function of aqueous solution temperature (Figure 1c). The two traces corresponding to the heating (open circles) and cooling (filled squares) processes are indistinguishable from each other within experimental uncertainty. It should also be pointed out that the spectral shift, as clearly seen in Figure 1c, is not linear with respect to the temperature change. It begins with either no or very little shift until the temperature reaches a characteristic value. While qualitatively similar shifts and broadening were also observed for the linear absorption spectra measured for both EO_2 and EO_3 at different temperatures, a hysteresis was found in both cases in the cooling processes even though the spectral changes are fully reversed eventually at the starting temperature of the corresponding heating-to-cooling circle (data not shown). The characteristic temperatures at which significant spectral shifts occur are obviously sample dependent. A more reliable comparison of these distinct characteristic temperatures can be made using the temperatures at which 10% of the overall shift occurs, which were estimated to be 47 °C, 51 °C, and 60 °C for EO_2, EO_3, and EO_4, respectively. We will consider these values as approximate LCSTs of these three polymers in the following.

When the aqueous solutions of these three polymers were heated to above their corresponding LCSTs, large aggregates form, as evident by the physical appearance change from clear solutions to turbid suspensions. Except for the red-shift and broadening, the linear absorption spectra remain essentially structureless as those observed below the LCSTs (see Figure 1a,b). These structureless spectra are strikingly distinct from the absorption spectra reported for the crystalline nanofibers formed through self-assembly of P3HT or poly(3-alkythiophene) in organic solvents, where vibronic transitions such as

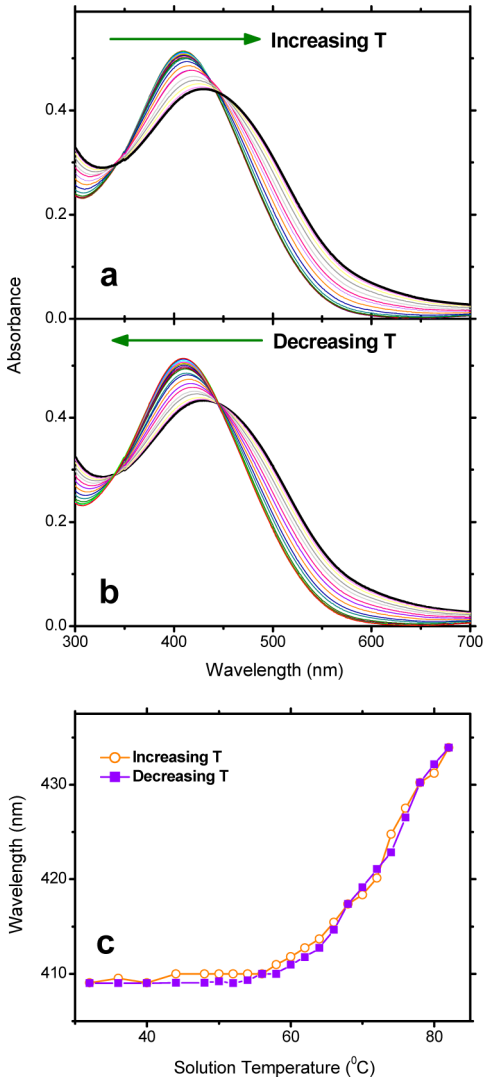

Figure 1. Linear absorption spectra recorded for EO_4 at different temperatures (32 °C to 80 °C) during heating (a) and cooling (b) segments. The spectra were measured every 4 °C from 32 °C to 48 °C and every 2 °C for higher temperatures. (c) Plot of the peak wavelengths of the absorption spectra measured during heating (open circles) and cooling (filled squares) versus aqueous solution temperature.

0−0 and 0−1 were clearly seen.[11,35−37] Upon closer visualization of the absorption spectra measured above the LCSTs (see Figure 2a for those recorded at 70 °C as an example), we further noticed that the spectral broadening increases with decreasing side-chain length. This result indicates that the shorter the side chain, the greater the spectral inhomogeneity.

In stark contrast to the strong temperature dependence of the absorption spectra, the corresponding fluorescence emission spectra show not only negligible spectral shifts but also very minor line-shape changes within experimental uncertainty. As an example, we show in Figure 2b the fluorescence emission spectra recorded for these polymers at 30 °C. However, the emission intensity decreases with increasing temperature, with a dramatic reduction observed at temperatures above the LCSTs. We further found that the Stokes shift decreases with increasing side-chain length; at 30 °C the values determined for EO_2, EO_3, and EO_4 are approximately 8300, 7900, and 7400 cm^{-1}, respectively.

dx.doi.org/10.1021/jp304526h | J. Phys. Chem. B 2012, 116, 14451−14460

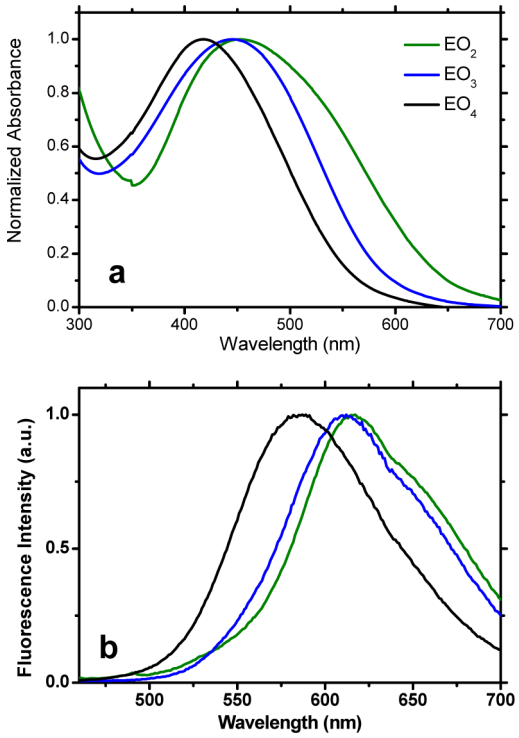

Figure 2. Linear absorption (a) and steady-state fluorescence emission spectra (b) recorded at 70 °C and 30 °C, respectively, for the EO_2 (dark green), EO_3 (blue), and EO_4 (black) polymers. All spectra are normalized at the peak absorbance or emission intensity.

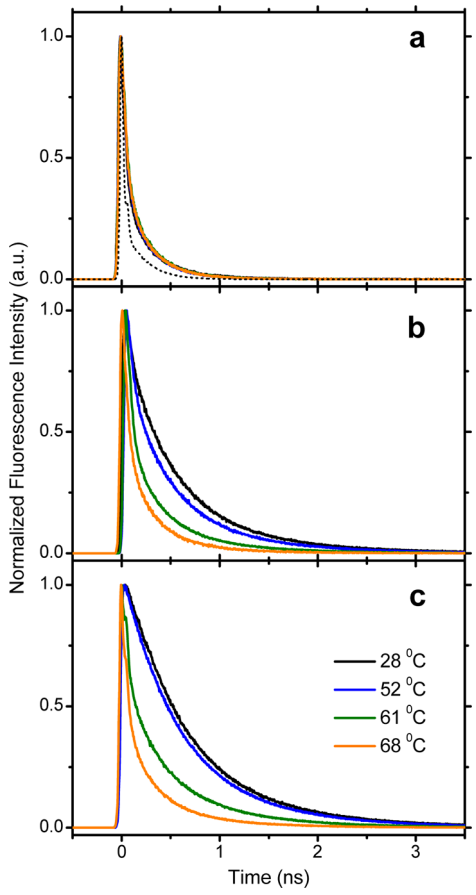

Figure 3. Isotropic fluorescence data collected at 28 °C, 52 °C, 61 °C, and 68 °C for EO_2 (a), EO_3 (b), and EO_4 (c). For ease of comparing their distinct decays, all the data have been normalized at the maximum intensities. The dotted line in plot a shows the IRF.

Moreover, because an increase of solution temperature causes red-shifted linear absorption spectra but does not affect the corresponding fluorescence emission spectra, this would lead to decreased Stokes shifts with increasing temperature for all three polymers.

Isotropic Fluorescence Decays at Different Temperatures. Representative time-resolved fluorescence data collected with the magic angle polarization at four different temperatures are shown in Figure 3. The isotropic fluorescence decays measured for both EO_3 and EO_4 exhibited significant acceleration when the sample solution temperature was raised to about 60 °C. The exact temperature appears dependent on the length of the side chain. For EO_3, an obviously faster decay was already noticeable at 52 °C, but this was not obvious for EO_4 until the temperature reached 61 °C. A further temperature increase led to an even faster decay, whereas below these temperatures (52 °C for EO_3 and 61 °C for EO_4) either no change or a minor effect was observed (Figure 3b,c). The temperatures at which clearly accelerated isotropic decays were observed for these two polymers correspond fairly well to their LCSTs. In contrast, the fluorescence data collected for EO_2 at all temperatures exhibit an essentially indistinguishable decay behavior from each other upon normalizing at the maximum fluorescence intensities, because all the decays were too rapid to be resolved with the available time resolution of our TCSPC apparatus (Figure 3a).

Quantitative analysis of the isotropic fluorescence decays were performed by employing a least-squares deconvolution fitting algorithm with explicit consideration of the finite instrumental response. Table 2 summarizes all the fitting parameters, including decay lifetimes, relative amplitudes, and reduced chi-squares (χ^2). Inclusion of the χ^2 values is intended to provide a quantitative measure of the fit quality. We found that the fluorescence decays measured for the EO_2 sample at all temperatures exhibited a biexponential decay behavior. The major component has a lifetime ranging from 28 to 33 ps and a relative amplitude of ~98%, whereas the minor component is characterized by a lifetime between 370 and 480 ps. The variation of the extracted lifetimes, especially for the major decay component, is likely to be caused by both sample temperature uncertainty and the limited signal-to-noise ratios of the experimental data. It should be emphasized that the similar fitting parameters extracted from these EO_2 data do not mean that this polymer is insensitive to temperature changes. Rather, the similarity arises from a very rapid decay at all temperatures, which is too fast to be resolved with our current experimental setup. Satisfactory fitting of the isotropic data collected for the EO_3 sample required a model function consisting of three exponents. The lifetime (relative amplitude) of the major decay component decreases from 50 ps (78%) at 28 °C to 31 ps (97%) at 68 °C, and the corresponding changes for the other two components are from 378 ps (15%) and 950 ps (7%) to 280 ps (2%) and 690 ps (1%), respectively. The isotropic fluorescence decays of the EO_4 sample are even more complicated, and the data collected at 589 nm can be satisfactorily fitted only with a model function consisting of four exponents. The lifetimes (relative amplitudes) of two major components vary from 29 ps (47%) and 126 ps (28%) at 28 °C to 10 ps (71%) and 44 ps (27%) at 68 °C. The

dx.doi.org/10.1021/jp304526h | J. Phys. Chem. B 2012, 116, 14451−14460

Table 2. Summary of the Lifetimes (τ_1–τ_4) and Relative Amplitudes (A_1–A_4) Extracted for the Isotropic Decays Measured at Different Temperatures through Deconvolution Data Fitting (χ^2 is the reduced chi-square, and T is the aqueous solution temperature)

polymer	T (°C)	τ_1 (ps)	A_1 (%)	τ_2 (ps)	A_2 (%)	τ_3 (ps)	A_3 (%)	τ_4 (ps)	A_4 (%)	χ^2
EO_2	29	28	98.8	477	1.2	–	–	–	–	0.952
	35	30	98.8	440	1.2	–	–	–	–	0.984
	44	32	98.7	404	1.3	–	–	–	–	1.001
	52	32	98.6	393	1.4	–	–	–	–	0.997
	61	33	98.3	376	1.7	–	–	–	–	1.086
	68	32	98.4	367	1.6	–	–	–	–	1.088
EO_3	28	50	78.1	378	15.2	947	6.7	–	–	1.141
	36	51	77.2	367	15.4	930	7.4	–	–	1.001
	44	49	78.3	352	14.5	907	7.2	–	–	1.149
	52	43	84.4	351	10.5	893	5.1	–	–	1.097
	61	33	94.6	359	3.7	866	1.7	–	–	1.054
	68	31	96.7	284	2.3	694	1.0	–	–	0.986
EO_4	29	29	47.0	126	27.7	536	17.1	1026	8.2	1.030
	36	27	46.7	118	28.5	505	16.0	986	8.8	1.073
	44	28	45.9	114	29.6	495	15.9	971	8.6	1.020
	52	29	45.1	109	30.7	481	15.2	944	9.0	1.021
	61	10	50.1	47	42.8	375	4.2	870	2.9	1.141
	68	10	71.1	44	26.6	386	1.6	851	0.7	1.002

corresponding slower decay components have lifetimes (relative amplitudes) ranging from 536 ps (17%) and 1.03 ns (8%) to 386 ps (2%) and 850 ps (1%).

By comparing the isotropic fluorescence decays measured at a given temperature, we further found that the length of the side chain plays a markedly large role on the excited-state relaxation dynamics of these polythiophene polymers. An increase of the side-chain length leads to significantly slower isotropic fluorescence decays (see, as an example, Figure 4a for the data recorded at 28 °C). This side-chain length effect can also be seen in a quantitative manner from a mean lifetime calculated using $\overline{\tau} = \sum_i \tau_i A_i / \sum_i A_i$, where τ and A represent the lifetimes and relative amplitudes extracted from the deconvolution data fitting and i is the number of exponents in a given fitting function. For the data collected at 44 °C, we obtained a mean lifetime of 36 ps for EO_2, 155 ps for EO_3, and 209 ps for EO_4. Furthermore, the decay rate difference observed for the three polymer samples decreases with increasing temperature, and at the highest sample temperature of our measurements (68 °C), the difference becomes only marginal (see Figure 4b). It is pertinent to point out that similar side-chain length effects were reported previously for amine-end-capped *p*-phenylenevinylene trimers with different side chains and end groups,[38] as well as their parent trimers 2,5-bis[(2-ethylhexyl)oxy]-*p*-phenylenevinylene and 2,5-bis[(3′-methylbutyl)oxy]-*p*-phenylenevinylene.[39] A noteworthy distinction between these previous reports and our current study is that the change of side-chain length influences mainly the fastest decay component in the former but the overall decay here. On the contrary, a significant reduction of fluorescence lifetime was observed when a thienylene-vinylene side chain of a polythiophene derivative was increased. This result was explained by assuming that more conformational defects were generated along the polymer main chain because of enhanced steric hindrance and strong twisting.[40]

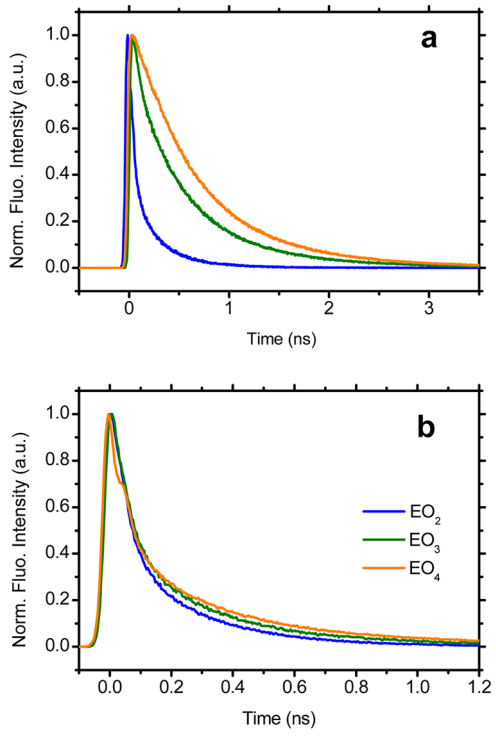

Figure 4. Comparison of isotropic fluorescence decays measured at (a) 28 °C and (b) 68 °C for EO_2, EO_3, and EO_4 samples. For ease of comparing their distinct decays, all the data have been normalized at the maximum intensities.

Time-Resolved Fluorescence Anisotropy. The isotropic fluorescence data described above are insensitive to the orientation changes of electronic transition dipole moments, which may arise from several rather rapid dynamical processes including (a) energy transfer from one conjugation segment to another either within the same polymer backbone or between different backbones, i.e., intra- or interchain excitation energy transfer, (b) the conformational changes of polymer backbones such as twisting or bending, and (c) overall polymer rotations in solution. To assess these changes directly in the time scales of their occurrence, we performed time-resolved fluorescence anisotropy measurements at the same detection wavelengths as employed for the isotropic experiments. Figure 5 shows the

dx.doi.org/10.1021/jp304526h | J. Phys. Chem. B 2012, 116, 14451–14460

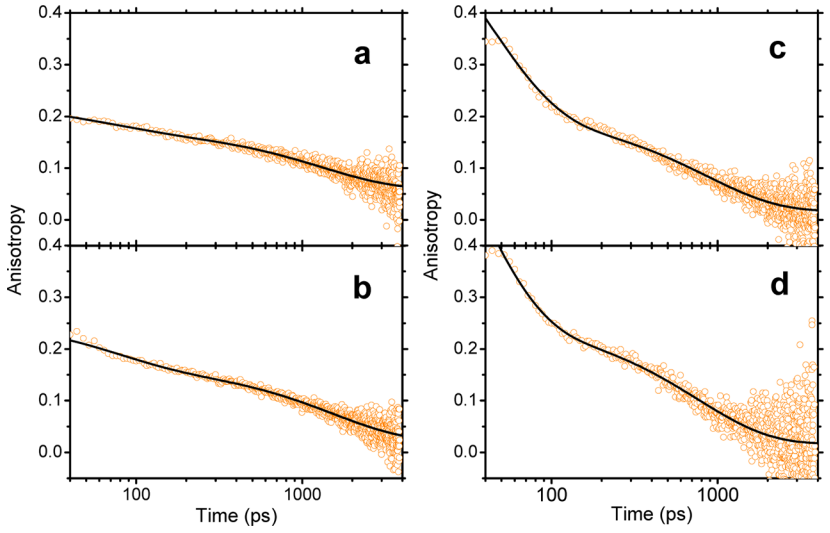

Figure 5. Time-resolved fluorescence anisotropic decays recorded for EO_4 at (a) 28 °C, (b) 44 °C, (c) 61 °C, and (d) 68 °C, respectively. The solid lines are biexponential decay fits. To avoid possible excitation light scattering, only the data after 40 ps are plotted.

anisotropic decays obtained for EO_4 at four different temperatures; the results obtained for EO_3 share substantial similarities (data not shown). At a low temperature such as at 28 °C, the anisotropies obtained for both EO_3 and EO_4 were characterized by an initial value of ∼0.2 and a relatively slow decay to a residual value of ∼0.1 at about 1.0 ns. A temperature increase led to several striking changes. First, the initial anisotropy increased substantially near and above the LCSTs, and at the highest temperature of our experiments (68 °C), the initial anisotropy almost reached the theoretical limit of 0.4, which is expected only when the absorption and emission transition dipole moments are parallel.[41] This observation suggests that a temperature-induced, remarkable change of the polymer backbone conformation occurs during aggregate formation. Following the collapse of the EO side chains, which causes the observed physical appearance change, such a conformational change of polymer backbones is obviously needed in order to bring different polymer molecules into close spatial proximity for aggregation. According to previous experimental and theoretical studies,[42−45] both the transition dipole moments associated with photon absorption and fluorescence emission should orient along the backbones. Consequently, the observed high initial anisotropy of ∼0.4 means that the polymer backbones must be highly ordered in the aggregates. Second, a fast decay component was clearly noticeable at 44 °C, which became more pronounced when the temperature was raised to 61 °C and 68 °C. The lifetime of this component shortened significantly with increasing temperature and was estimated to be 36 ps at 68 °C. Note that this lifetime was extracted without deconvolution using the IRF, and therefore it should be viewed as a rough estimate. This rapid anisotropic decay can be straightforwardly assigned to an interchain energy transfer process, i.e., from one polymer chain to another within the same aggregate. This interchain transfer is possible only when the polymer chains are spatially adjacent, which can further explain why no such a decay was found in the solubilized case at temperatures below the LCSTs. Third, the subsequent slower decay also accelerated clearly near and above the LCSTs, which varies from roughly few nanoseconds at 28 °C to about 870 ps at 68 °C. Furthermore, at any given temperature, the anisotropic decays proceed until the corresponding isotropic fluorescence signals cease. As already seen from the isotropic decays, the anisotropic data recorded for EO_2 again are an exception. Due to the rapid excited-state relaxation, the fluorescence signals at delay times greater than 200 ps are low for any combination of the excitation and emission polarizations, and therefore the anisotropy data show poor signal-to-noise ratios. Nevertheless, these data exhibit initial anisotropies between 0.25 and 0.3, but no clear trend with temperature changes can be ascertained with confidence.

■ DISCUSSION

The key findings of our time-resolved fluorescence experiments can be summarized as follows. First, the isotropic fluorescence decay depends strongly on the polymer side-chain length. An increase of the side-chain length leads to not only significantly slower decay rates but also more complex decay behavior, which is evident from the greater number of exponents needed for satisfactory description of the decay. Second, the fluorescence decays of EO_3 and EO_4 measured near and above their LCSTs depend markedly on the aqueous solution temperature, manifested by more rapid decay rates at higher temperatures. However, the complexity of the decay behavior remains unchanged for each polymer. No such temperature dependence could be resolved for EO_2 owing to its extremely rapid decay with respect to our available time resolution at all measured temperatures. Third, a similar temperature effect was also observed for the anisotropic decays obtained for EO_3 and EO_4, which are characterized by clearly temperature-dependent initial anisotropies and decay time scales. Of particular interest is the observation of an initial anisotropy of ∼0.4 above the LCSTs, which is only expected when the transition dipole moments associated with photon absorption and fluorescence emission are parallel. This result suggests that the polymer chains within the aggregates are highly ordered. Finally, for either polymer at any given temperature, the anisotropic decay was found to persist for essentially the same time as the corresponding isotropic decay. In the following, we will discuss separately the effects of side-chain length and aqueous solution temperature on time-resolved fluorescence isotropic decays, as well as how the aggregates formed near and above the LCSTs

dx.doi.org/10.1021/jp304526h | J. Phys. Chem. B 2012, 116, 14451−14460

differ from those crystalline polythiophene nanofibers discovered previously in organic solvents.

Side-Chain Length Effect. Because the hydrophilic side chains collapse and large aggregates form near and above the LCSTs presumably because of a change in the hydrogen-bonding interactions with water molecules, we will restrict our discussion to only the data collected below the LCSTs to ensure that the polymer chains are homogeneously dispersed in water. In this case, the favorable hydrogen-bonding interactions between the hydrophilic side chains and water molecules must be strong enough to balance the unfavorable interactions between water molecules and the polymer backbones,[28] which may adopt either an extended or a twisted conformation. While a highly twisted, coiled conformation has been reported for a nonionic water-soluble conjugated polymer, poly[2,5-bis-(diethylaminetetraethylene glycol)phenylene vinylene] in water,[26] we do not expect that any of the three polymers examined in this work will adopt such a conformation. This is because thiophene-based polymers, just like other conjugated polymers, usually adopt rodlike conformation due to their extensive main-chain conjugation.[46,47] Absence of such coiled conformations is further supported by our time-resolved fluorescence anisotropy data. If such coiled conformations with tight backbone folding were formed, different segments of the same polymer backbone would become spatially close and then intrachain excitation energy transfer could occur.[48] Because this transfer takes typically a few tens of picoseconds,[18] its occurrence would lead to fast depolarization and the anisotropy should reach zero in a short time. This is clearly inconsistent with the much slower anisotropy decays we observed (Figure 5), which proceed until the corresponding isotropic decays end. On the basis of these arguments, we will consider only extended backbone conformations in the following discussion.

It has been widely accepted that, upon photoexcitation, conjugated polymers generally undergo conformational changes, such as from aromatic toward quinoidal geometries.[49−51] Consequently, similar changes are also expected in the relaxation process from the electronic excited state to the corresponding ground state. The relaxation time scales should therefore depend on how fast these conformational changes take place, which in turn depend on the rigidness of the backbones and the strength of the hydrogen-bonding interactions between the attached hydrophilic side chains and the water molecules. Given the same backbones, longer side chains and concomitant stronger hydrogen-bonding interactions should make these conformational changes more difficult and consequently slow down the excited-state relaxation as compared to polymers with shorter side chains. As a result, we can expect slower fluorescence decay with increasing side-chain length, which is qualitatively consistent with our experimental observations. This consideration can also explain why the isotropic decays become more complex with lengthening the side chain. Because of the stronger hydrogen-bonding interactions, the longer side chains will be capable of accommodating a greater number of backbone conformations. According to previous experimental[38,39,52−57] and theoretical studies,[58−60] the spectroscopic and photophysical properties of conjugated polymers depend strongly on their backbone conformations. This would indicate that presence of different number of backbone conformations should give rise to distinct excited-state decay behavior. On the basis of the consideration given above, we attribute the observed isotropic decays below the LCSTs to the conformational relaxation of their backbones in their electronically excited first singlet states.

So far, we have assumed that the solubilized polymer molecules exist mainly as single chains with no aggregation. However, this may not be true in view of the shoulder on the red-side of the EO_2 and EO_3 emission spectra (Figure 2b). Formation of small aggregates such as dimers or trimers will not alter the physical appearance of the aqueous solutions, but could be visible in the fluorescence emission. Presence of these small aggregates could further lead to an accelerated isotropic decay as observed previously for poly[3-(4-octylphenyl)-2,2́-bithiophene].[61] The absence of such a shoulder in EO_4 emission is most probably because this polymer has much higher solubility than either EO_3 or EO_2 and therefore has the least tendency of forming aggregates. An examination of the relative contents of these small aggregates and their precise influence on the fluorescence isotropic decays requires more detailed study with detection of time-resolved fluorescence data at multiple wavelengths and for different solution concentrations in combination with global lifetime analyses. Such a study, however, is beyond the scope of this work.

Temperature Effect. We now turn to the temperature effect. As shown in Figure 3b,c, the isotropic decays of both EO_3 and EO_4 clearly become faster when the solution temperature was raised to near or above their LCSTs. At these temperatures, the hydrophilic side chains collapse and should no longer impact the excited-state relaxation. Upon aggregation, the spatially adjacent polymer chains will enable interchain energy transfer from the excited molecules to those unexcited ones. This transfer should accelerate as the chain ordering improves with rising temperature, which is evident by the increased initial anisotropies (see Figure 5). An improved ordering may bring different polymer chains even closer and/or give rise to a more favorable orientation for the energy transfer. Occurrence of this interchain transfer and its acceleration with temperature can qualitatively explain the temperature effect observed.

The change of chain ordering in the aggregates can further affect the relaxation of the excited polymers to their ground states due to the involvement of distinct conformational changes at different temperatures. Here, the temperature change should affect mainly the ground-state conformations as judged from the large and continuous shift and broadening of the linear absorption spectra with rising temperature. According to the density functional theory calculations of Zade and Bendikov, a polymer band gap is strongly dependent on chain twisting.[59] Thus, a red-shifted linear absorption spectrum, or equivalently a reduced band gap, must be accompanied by a conformational change of polymer chain. This is further supported by the substantial increase of initial anisotropies observed for EO_3 and EO_4 near or above their LCSTs. A higher initial anisotropy means a smaller angle between the transition dipole moments associated with absorption and emission and thus more similar conformations in the excited-state and ground state. Consequently, the relaxation should be faster at a higher temperature, as less conformational change is needed. This temperature-dependent relaxation process can be visualized through a schematic description depicted in Figure 6. At a lower temperature, different polymer chain conformations are represented by clearly distinct potential energy curves with relatively larger displacement between the E_0 and E_1 minima. Both photon absorption and fluorescence emission, depicted by vertical

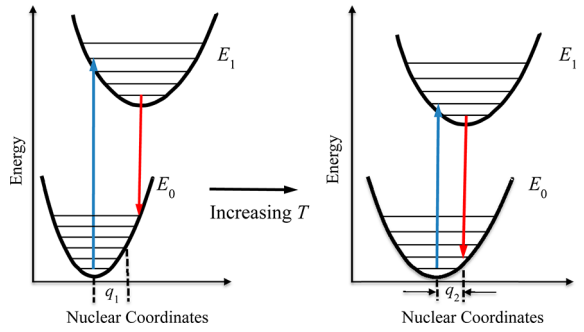

Figure 6. Schematic model describing the temperature-dependence of excited-state relaxation dynamics in water-soluble polythiophene polymers. E_0 and E_1 represent the ground state and first singlet excited state, and q_1 and q_2 denote the relative shifts of their potential energy curves. The vertical arrows depict photon absorption and fluorescence emission. The corresponding energy differences or Stokes shifts decrease when the two potential energy curves are more similar and possess a smaller q displacement between their minima.

arrows, will be accompanied by a substantial conformational change. As a result, a larger Stokes shift as observed experimentally is expected. At a higher temperature, the two curves share more similarities and a smaller displacement, and therefore little conformational change is required between the photon absorption and fluorescence emission transitions. The corresponding Stokes shift reduces as well, which is again consistent with our experimental data. We would like to emphasize that this is again a conformational relaxation, but from an excited state to a ground state with a temperature-dependent chain conformation.

The occurrence of this interchain energy transfer and/or conformational relaxation at temperatures near and above the LCST was also supported by the isotropic data that were collected for EO_4 at 620 nm (data not shown), which is located at the low energy region of the steady-state fluorescence emission spectrum (Figure 2b). Satisfactory fitting of the data measured at 61 °C and 68 °C is only possible when a rise component is also included in the model function, and then the lifetimes extracted are 11 and 14 ps, respectively. This lifetime corresponds fairly well to the fastest 10 ps decay component resolved from the data collected at 589 nm at the same temperatures (see the last two rows in Table 2). No such rise component could be resolved from the data measured below the LCST. However, based on these data alone, we can assign neither this rapid rise seen at 620 nm nor its corresponding decay at 589 nm exclusively to an interchain transfer or a conformational relaxation because both these dynamical processes can result in the same kinetic rise and decay. A possible way of distinguishing these processes is to vary the viscosity of the aqueous solution and thus slow down the conformational change, which will be an interesting topic for future study.

Obviously, our argument about the temperature influence on the relaxation of an excited polymer to its ground state is valid only when the interactions between the polymer chains in the same aggregate are sufficiently weak so that they behave as individual molecules. As will be discussed in the following subsection, the weak interactions are indeed supported by the structureless absorption spectra seen near and above the LCSTs.

Comparison of the Aggregates Formed near and above LCSTs with Crystalline Polythiophene Nanofibers. The high initial anisotropy of ~0.4 observed for EO_3 and EO_4 above their LCSTs indicates that the polymer chains became highly ordered in contrast to the randomly oriented chains in the solubilized case below the LCSTs. This may not be surprising in view of the long-range structural order discovered for the polythiophene nanfibers in organic solvents.[11,35,37,62] However, their linear absorption spectra are strikingly distinct. While vibronic transitions such as 0−0 and 0−1 are clearly evident in the nanofibers,[11,35−37] these transitions are entirely absent in the aggregates formed near and above LCSTs here (see Figure 2a). We believe that these distinct spectral features arise from the different nature of interchain interactions: excitonic in the nanofibers versus van der Waals in the aggregates. Owing to the presence of side chains and possibly some "residual" water molecules, the aggregates may be somewhat "swollen", similar to those suspended nanofibers prior to solvent evaporation.[28] The weaker interactions in the latter case ensure that the aggregates can be converted entirely into the solubilized form even when only a small temperature drop to below the LCSTs occur and therefore produce the fully reversible linear absorption spectra as observed experimentally.

CONCLUSIONS

In this paper, we report synthesis of three thermoresponsive poly(3-oligo(ethylene oxide)) thiophenes with different side-chain lengths and LCSTs. The linear absorption spectra of these polymers exhibit fully reversible changes (spectral shift and broadening) with variation of the aqueous solution temperature, whereas their steady-state fluorescence emission spectra show negligible shifts in combination with very minor line-shape changes. Consequently, a decrease in the Stokes shifts with increasing temperature was observed for all three polymers. Near and above the LCSTs, the aggregates formed were further found to exhibit no vibronic transitions in contrast to those observed for crystalline polythiophene nanofibers. We believe that this difference arises from the distinct nature of interchain interactions in the two cases.

By application of picosecond time-resolved fluorescence spectroscopy, we demonstrated that the excited-state relaxation dynamics of these polymers in aqueous solution depend strongly on the side-chain length and temperature. With lengthening of the side chain, the isotropic fluorescence signals exhibit not only remarkably slower decays but also an increasingly complex decay behavior. The differences between these isotropic decays decrease gradually with increasing temperature and become minimal at the highest temperature of our measurements (68 °C), but the complexity of the decay behavior remains unchanged for each polymer. On the other hand, significant acceleration of the isotropic decays was observed for both EO_3 and EO_4 when the aqueous solutions were heated to their LCSTs, 51 °C for EO_3 and 60 °C for EO_4, and above; at these temperatures, large aggregates form as evident by the physical appearance change from clear solutions to turbid suspensions. We attribute the observed side-chain length effect to the conformational relaxation of the polymer backbones. The temperature effect observed near and above the LCSTs, on the other hand, arises from an interchain energy transfer between the spatially adjacent chains in the aggregates and a change in the excited-state relaxation owing to the involvement of distinct chain conformations in the ground state. Both processes should accelerate with increasing temperature. A particularly interesting observation is the

remarkable changes of time-resolved fluorescence anisotropies near and above LCSTs, which are manifested by a substantial increase of initial values from ~0.2 to 0.4 in combination with the appearance of a pronounced fast anisotropic decay component with a shortest lifetime estimated to be 36 ps. These different initial anisotropies provide direct evidence for a temperature-induced change of polymer chain conformations in the aggregates, especially for the formation of highly ordered chains at the highest temperature of our time-resolved experiments (68 °C). No clear temperature dependence could be identified with confidence for either isotropic or anisotropic decays collected for EO_2 due to our limited instrumental time resolution.

AUTHOR INFORMATION

Corresponding Author

*(Y.-Z.M.) Phone: 865-574-7213. Fax: 865-574-8363. E-mail: may1@ornl.gov. (K.H.) Phone: 865-574-4974. Fax: 865-574-1753. E-mail: hongkq@ornl.gov.

Notes

The authors declare no competing financial interest.

ACKNOWLEDGMENTS

This manuscript was authored by UT-Battelle, LLC, under Contract No. DE-AC05-00OR22725 with the U.S. Department of Energy. Research was sponsored by the Laboratory Directed Research and Development Program of ORNL, managed by UT-Battelle, LLC, for the U.S. Department of Energy (Y.-Z.M., FY2010, 2011), and the Division of Chemical Sciences, Geosciences, and Biosciences, Office of Basic Energy Sciences, U.S. Department of Energy (Y.-Z.M. and R.W.S., FY2012). The research conducted at the Center for Nanophase Materials Sciences of Oak Ridge National Laboratory is sponsored by the Scientific User Facilities Division, Office of Basic Energy Sciences, U.S. Department of Energy.

REFERENCES

(1) Brinkmann, M. *J. Polym. Sci., Part B: Polym. Phys.* **2011**, *49*, 1218−1233.
(2) Bernius, M. T.; Inbasekaran, M.; O'Brien, J.; Wu, W. S. *Adv. Mater.* **2000**, *12*, 1737−1750.
(3) Osaka, I.; McCullough, R. D. *Acc. Chem. Res.* **2008**, *41*, 1202−1214.
(4) Ohmori, Y.; Uchida, M.; Muro, K.; Yoshino, K. *Jpn. J. Appl. Phys.* **1991**, *30*, L1938−L1940.
(5) Ohmori, Y.; Morishima, C.; Uchida, M.; Yoshino, K. *Jpn. J. Appl. Phys.* **1992**, *31*, L568−L570.
(6) Braun, D.; Gustafsson, G.; McBranch, D.; Heeger, A. J. *J. Appl. Phys.* **1992**, *72*, 564−568.
(7) Nguyen, L. H.; Hoppe, H.; Erb, T.; Gunes, S.; Gobsch, G.; Sariciftci, N. S. *Adv. Funct. Mater.* **2007**, *17*, 1071−1078.
(8) Faridbod, F.; Ganjali, M. R.; Dinarvand, R.; Norouzi, P. *Sensors* **2008**, *8*, 2331−2412.
(9) Pang, Y. H.; Li, X. Y.; Ding, H. L.; Shi, G. Y.; Jin, L. T. *Electrochim. Acta* **2007**, *52*, 6172−6177.
(10) Ma, W.; Yang, C.; Gong, X.; Lee, K.; Heeger, A. J. *Adv. Funct. Mater.* **2005**, *15*, 1617−1622.
(11) Baghgar, M.; Labastide, J.; Bokel, F.; Dujovne, I.; McKenna, A.; Barnes, A. M.; Pentzer, E.; Emrick, T.; Hayward, R.; Barnes, M. D. *J. Phys. Chem. Lett.* **2012**, *3*, 1674−1679.
(12) Spano, F. C. *Acc. Chem. Res.* **2010**, *43*, 429−439.
(13) Spano, F. C. *J. Chem. Phys.* **2005**, *122*, 234701.
(14) Banerji, N.; Cowan, S.; Vauthey, E.; Heeger, A. J. *J. Phys. Chem. C* **2011**, *115*, 9726−9739.
(15) Busby, E.; Carroll, E. C.; Chinn, E. M.; Chang, L.; Moulé, A. J.; Larsen, D. S. *J. Phys. Chem. Lett.* **2011**, *2*, 2764−2769.
(16) Labastide, J. A.; Baghgar, M.; Dujovne, I.; Venkatraman, B. H.; Ramsdell, D. C.; Venkataraman, D.; Barnes, M. D. *J. Phys. Chem. Lett.* **2011**, *2*, 2089−2093.
(17) Wells, N. P.; Boudouris, B. W.; Hillmyer, M. A.; Blank, D. A. *J. Phys. Chem. C* **2007**, *111*, 15404−15414.
(18) Scheblykin, I. G.; Yartsev, A.; Pullerits, T.; Gulbinas, V.; Sundström, V. *J. Phys. Chem. B* **2007**, *111*, 6303−6321.
(19) Banerji, N.; Seifter, J.; Wang, M.; Vauthey, E.; Wudl, F.; Heeger, A. J. *Phys. Rev. B* **2011**, *84*, 075206.
(20) Ayzner, A. L.; Doan, S. C.; de Villers, B. T.; Schwartz, B. J. *J. Phys. Chem. Lett.* **2012**, *3*, 2281−2287.
(21) Marsh, R. A.; Hodgkiss, J. M.; Albert-Seifried, S.; Friend, R. H. *Nano Lett.* **2010**, *10*, 923−930.
(22) Guo, J.; Ohkita, H.; Benten, H.; Ito, S. *J. Am. Chem. Soc.* **2010**, *132*, 6154−6164.
(23) Howard, I. A.; Mauer, R.; Meister, M.; Laquai, F. *J. Am. Chem. Soc.* **2010**, *132*, 14866−14876.
(24) Gaylord, B. S.; Heeger, A. J.; Bazan, G. *J. Am. Chem. Soc.* **2003**, *125*, 896−900.
(25) Krishna, G.; Thalluri, V. V.; Biolsée, J.-C.; Gadisa, A.; Parchine, M.; Boonen, T.; D'Haen, J.; Boyukbayram, A. E.; Vandenbergh, J.; Cleij, T. J.; Lutsen, L.; Vanderzande, D.; Manca, J. *Sol. Energy Mater. Sol. Cells* **2011**, *95*, 3262−3268.
(26) Xu, Z.; Tsai, H.; Wang, H.-L.; Cotlet, M. *J. Phys. Chem. B* **2010**, *114*, 11746−11752.
(27) Schild, H. G. *Prog. Polym. Sci.* **1992**, *17*, 163−249.
(28) Lutz, J.-F.; Weichenhan, K.; Akdemir, Ö.; Hoth, A. *Macromolecules* **2007**, *40*, 2503−2508.
(29) Lutz, J.-F.; Hoth, A.; Schade, K. *Des. Monomers Polym.* **2009**, *12*, 343−353.
(30) Zhang, Y.; Cremer, P. S. *Annu. Rev. Phys. Chem.* **2010**, *61*, 63−83.
(31) Lessard, D. G.; Ousalem, M.; Zhu, X. X.; Eisenberg, A.; Carreau, P. J. *J. Polym. Sci., Part B: Polym. Phys.* **2003**, *41*, 1627−1637.
(32) Aseyev, V.; Hietala, S.; Laukkanen, A.; Nuopponen, M.; Confortini, O.; Du Prez, F. E.; Tenhu, H. *Polymer* **2005**, *46*, 7118−7131.
(33) Kujawa, P.; Aseyev, V.; Tenhu, H.; Winnik, F. M. *Macromolecules* **2006**, *39*, 7686−7693.
(34) Kiriy, A.; Senkovskyy, V.; Sommer, M. *Macromol. Rapid Commun.* **2011**, *32*, 1503−1517.
(35) Oosterbaan, W. D.; Vrindts, V.; Berson, S.; Guillerez, S.; Douhéret, O.; Ruttens, B.; D'Haen, J.; Adriaensens, P.; Manca, J.; Lutsen, L.; Vanderzande, D. *J. Mater. Chem.* **2009**, *19*, 5424−5435.
(36) Sun, S.; Salim, T.; Wong, L. H.; Foo, Y. L.; Boey, F.; Lam, Y. M. *J. Mater. Chem.* **2011**, *21*, 377−386.
(37) Roehling, J. D.; Arslan, I.; Moulé, A. J. *J. Mater. Chem.* **2012**, *22*, 2498−2506.
(38) Di Paolo, R. E.; Gigante, B.; Esteves, M. A.; Pires, N.; Santos, C.; Lameiro, M. H.; Seixas de Melo, J.; Burrows, H. D.; Maçanita, A. L. *ChemPhysChem* **2008**, *9*, 2214−2220.
(39) Di Paolo, R. E.; Seixas de Melo, J.; Pina, J.; Burrows, H. D.; Morgado, J.; Maçanita, A. L. *ChemPhysChem* **2007**, *8*, 2657−2664.
(40) Meng, K.; Ding, Q.; Wang, S.; He, Y.; Li, Y.; Gong, Q. *J. Phys. Chem. B* **2010**, *114*, 2602−2606.
(41) van Amerongen, H.; Struve, W. S. *Methods Enzymol.* **1995**, *246*, 259−283.
(42) Langeveld-Voss, B. M. W.; Janssen, R. A. J.; Meijer, E. W. *J. Mol. Struct.* **2000**, *521*, 285−301.
(43) Grage, M. M.-L.; Pullerits, T.; Ruseckas, A.; Theander, M.; Inganäs, O.; Sundström, V. *Chem. Phys. Lett.* **2001**, *339*, 96−102.
(44) Grage, M. M.-L.; Zaushitsyn, Y.; Yartsev, A.; Chachisvilis, M.; Sundström, V.; Pullerits, T. *Phys. Rev. B* **2003**, *67*, 205207.
(45) Beenken, W. J. D.; Pullerits, T. *J. Chem. Phys.* **2004**, *120*, 2490−2495.
(46) Lee, C. K.; Hua, C. C.; Chen, S. A. *J. Chem. Phys.* **2012**, *136*, 084901.

(47) Huang, Y.; Cheng, H.; Han, C. C. *Macromolecules* **2011**, *44*, 5020−5026.
(48) Collini, E.; Scholes, G. D. *Science* **2009**, *323*, 369−373.
(49) Tretiak, S.; Saxena, A.; Martin, R. L.; Bishop, A. R. *Phys. Rev. Lett.* **2002**, *89*, 097402.
(50) Sun, Y.; Li, Y.; Li, Y.; Ma, F. *Comput. Mater. Sci.* **2007**, *39*, 673−677.
(51) Casado, J.; Miller, L. L.; Mann, K. R.; Pappenfus, T. M.; Higuchi, H.; Ortí, E.; Milián, B.; Pou-AméRigo, R.; Hernández, V.; López Navarrete, T. L. *J. Am. Chem. Soc.* **2002**, *124*, 12380−12388.
(52) Nguyen, T.-Q.; Doan, V.; Schwartz, B. J. *J. Chem. Phys.* **1999**, *110*, 4068−4078.
(53) Belletête, M.; Mazerolle, L.; Desrosiers, N.; Leclerc, M.; Durocher, G. *Macromolecules* **1995**, *28*, 8587−8597.
(54) Belletête, M.; Morin, J.-F.; Beaupré, S.; Ranger, M.; Leclerc, M.; Durocher, G. *Macromolecules* **2001**, *34*, 2288−2297.
(55) Pina, J.; Seixas de Melo, J.; Burrows, H. D.; Maçanita, A. L.; Galbrecht, F.; Bünnagel, T.; Scherf, U. *Macromolecules* **2009**, *42*, 1710−1719.
(56) Pina, J.; Seixas de Melo, J.; Burrows, H. D.; Bünnagel, T. W.; Dolfen, D.; Kudla, C. J.; Scherf, U. *J. Phys. Chem. B* **2009**, *113*, 15928−15936.
(57) Sugimoto, T.; Ebihara, Y.; Ogino, K.; Vacha, M. *ChemPhysChem* **2007**, *8*, 1623−1628.
(58) De Leener, C.; Hennebicq, E.; Sancho-Garcia, J.-C.; Beljonne, D. *J. Phys. Chem. B* **2009**, *113*, 1311−1322.
(59) Zade, S. S.; Bendikov, M. *Chem.—Eur. J.* **2007**, *13*, 3688−3700.
(60) Scherf, U. *J. Mater. Chem.* **1999**, *9*, 1853−1864.
(61) Ruseckas, A.; Namdas, E. B.; Theander, M.; Svensson, M.; Yartsev, A.; Zigmantas, D.; Andersson, M. R.; Inganäs, O.; Sundström, V. *J. Photochem. Photobiol., A* **2001**, *144*, 3−12.
(62) Merlo, J. A.; Frisbie, C. D. *J. Phys. Chem. B* **2004**, *108*, 19169−19179.